Clay Minerals (2023), **58**, 26–37
doi:10.1180/clm.2023.9

CAMBRIDGE UNIVERSITY PRESS

Article

Plastic behaviour of clay materials for the manufacture of fast-drying red ceramics

Vitor de Souza Nandi, Alexandre Zaccaron, Fabiano Raupp-Pereira, Sabrina Arcaro, Adriano Michael Bernardin and Oscar Rubem Klegues Montedo*

Universidade do Extremo Sul Catarinense (UNESC), Programa de Pós-graduação em Ciência e Engenharia de Materiais (PPGCEM), Avenida Universitária, 1105–88806-000, Criciúma (SC), Brazil

Abstract

Fast drying (~60 min) is useful for optimizing production processes by increasing productivity and reducing costs and environmental impacts, especially in red ceramic industries in Brazil. However, suitable clays are necessary and, currently, studies focused on the plastic behaviour of clays with compositions suitable for extrusion, especially for fast drying, are scarce. Therefore, in this study, three different clays from the same mineral deposit were studied for producing clay-based structural products *via* fast drying. The clays were characterized according to their chemical, mineralogical and thermal properties, particle size, cation-exchange capacity, specific surface area and open pore volume distribution. Ten formulations were developed using a simplex-centroid mixture design of experiments and their plasticity index (PI) values were determined. The response surfaces of the formulations were evaluated according to their PI, while the formation characteristics were determined according to their extrusion workability factor values. Formulations F5 (50.0 wt.% yellow clay and 50.0 wt.% green clay) and F8 (66.6 wt.% yellow clay, 16.7 wt.% grey clay and 16.7 wt.% green clay; PI = 15.5–16.6%) displayed optimal extrusion properties, followed by formulations F7 (33.3 wt.% yellow clay, 33.3 wt.% grey clay and 33.3 wt.% green clay) and F10 (16.7 wt.% yellow clay, 16.7 wt.% grey clay and 66.6 wt.% green clay; PI = 13.8–14.2%), which are within acceptable extrusion index values. Thus, the chosen formulations have significant potential for use in the manufacture of fast-drying red ceramics.

Keywords: Argillite, clay mineral, extrusion, plasticity, red ceramic

(Received 21 July 2022; revised 21 March 2023; Accepted Manuscript online: 30 March 2023; Associate Editor: M. Dondi)

Brazil is one of the largest producers and consumers of clay construction materials. According to the Secretariat of Geology, Mining, and Mineral Processing (MME, 2022), ~170 million tons of clay are used annually in the structural red ceramic industry in Brazil. Natural clays are essential in the red ceramic industry (Jemaï *et al.*, 2015). In particular, sealing and structural blocks made of red clays are the most widely used and versatile products in Brazil's construction industry (Zaccaron *et al.*, 2021). This is ascribed to the favourable characteristics of clays, including their availability, mechanical, physical and thermal durability, unique acoustic properties and weathering resistance (Deboucha & Hashim, 2011; Shakir & Mohammed, 2013; Ukwatta *et al.*, 2015; Kazmi *et al.*, 2016; Muñoz *et al.*, 2016).

Due to their plasticity, clay-based materials are suitable for extrusion moulding; however, the more plastic the material, the greater the water content necessary to achieve the workable plasticity, which may lead to the emergence of drying cracks and hence reductions in mechanical strength (Andrade *et al.*, 2011).

For ceramic purposes, clay deposits have a wide geographical distribution throughout Brazil. This can be attributed to the extensive sedimentary covering of the Brazilian geological substrate, which includes Phanerozoic basins and Cenozoic deposits that form significant residual weathering covers through their geomorphological evolution. In a geological context, two main types of deposits are distinguished: quaternary and sedimentary basin clays (Schaefer *et al.*, 2008; Cabral Junior *et al.*, 2012).

Quaternary clays are associated with deposits that fill valley bottoms and coastal plains, forming lenticular deposits with thicknesses in the range of metres that occupy hectares. Sedimentary basin clays comprise shales, argillites, siltstones, rhythmites and pelites, which are called 'taguas' generically. These rocks contain clay minerals of the illite group predominantly, which are rich in potassium, an alkali metal that decreases their sintering temperature. In addition, tagua rocks contain large amounts of ferruginous materials, which facilitate the sintering process and provide reddish firing colours (Cabral Júnior *et al.*, 2008).

To optimize the processing of red ceramics, it is necessary to know the chemical and mineralogical characteristics of the composition used to manufacture the product, amongst other factors. Plasticity is a key property (Vasconcellos *et al.*, 2019). Plasticity is related to the deformation of a body that is retained after stress relief when subjected to a certain external force (Aghayev & Küçükuysal, 2018). It is affected by many of the physicochemical parameters of clays, especially their mineralogy, particle-size distribution and the presence of soluble salts and organic matter.

***Corresponding author:** Rubem Klegues Montedo, Email: okm@unesc.net
Cite this article: Nandi VdeS, Zaccaron A, Raupp-Pereira F, Arcaro S, Bernardin AM, Montedo ORK (2023). Plastic behaviour of clay materials for the manufacture of fast-drying red ceramics. *Clay Minerals* **58**, 26–37. https://doi.org/10.1180/clm.2023.9

The plastic characteristics of clays and therefore their workability during the forming process constitute some of the main requirements for their use in the manufacture of red ceramics (Marsigli & Dondi, 1997).

Given its complexity, the plasticity of clays has been investigated empirically using various test methodologies. In the red ceramics sector, the most widespread methods used are those of Atterberg and Pfefferkorn (Marsigli & Dondi, 1997). Several studies have been carried out in recent years on the interpretation of the plastic behaviours of clays using the Atterberg and Pfefferkorn methods (Crozetta *et al.*, 2016; Karakan & Demir, 2018, 2020; Karakan *et al.*, 2020; Karakan, 2022a, 2022b) and the indentation method.

Doménech *et al.* (1994) evaluated the plasticity of ceramic compositions using the indentation method and determined that the liquid limit (LL) and the plastic limit (PL) can be obtained for consistencies (applied forces) of 1 and 46 N, respectively. A comparison between the indentation method and the Pfefferkorn method showed that the former is reliable and more accurate than the latter, in addition to it being more practical in its application (Modesto & Bernardin, 2008).

Red ceramic products mainly include roof tiles, structural blocks and bricks, which have high plasticity, requiring considerable amounts of water for their shaping through extrusion. In the subsequent drying process, water is removed from the moulded material using significant amounts of thermal energy (Inocente *et al.*, 2017; Nield & Simmons, 2019; Nicolas *et al.*, 2020). Nevertheless, some clays have no appreciable plasticity and therefore do not require considerable amounts of water for extrusion.

The drying of ceramic materials has been studied extensively in the past (Toei, 1985; Toei *et al.*, 1994; Ben Mabrouk & Belghith, 1995; Ketelaars *et al.*, 1995; Zanden, 1996) in an attempt to optimize this process. These studies, however, were limited by their slow drying cycles (>10 h). Recent studies have focused on shorter drying times (<3 h), with an emphasis mainly on the nature of the raw materials used (Zaccaron *et al.*, 2021, 2022).

Fast drying (~60 min) is most often used for ceramic materials with low water contents (typically <8%). This means that the use of fast drying for red ceramics is not simple, as the highly plastic clays used in red ceramics have water contents that exceed 20% and can reach 25%. Thus, the removal of water at high heating rates may lead to the formation of drying cracks, which reduce the mechanical strength of the material or even render it unusable. Thus, the use of fast drying in the red ceramics sector requires the study of clays and compositions that allow for adequate extrusion whilst only requiring short drying times (<120 min) for the reduction of water without promoting the appearance of permanent defects in the dried sections.

Hence, the study of clay-based ceramic formulations for the manufacture of red ceramics using the fast-drying process should include careful analysis of the plasticity of the clay by means of its mineralogical composition and the nature and granulometric distribution of its particles. This approach may allow the elimination of water at greater evaporation rates without causing permanent defects in the material.

Although the physicochemical and mineralogical properties of the clays used in red ceramic formulations could facilitate the mixing process and minimize losses incurred during formation and thermal treatment (drying and firing), studies focused on the plastic behaviour of clays to determine those compositions suitable for extrusion, especially for fast-drying processes, remain scarce. This study aims to analyse the plasticity behaviour of various clays used in the fast-drying production of red ceramics.

Materials and methods

Three clays, namely yellow clay (AM), grey clay (AC) and green clay (AV), were collected from a quarry located 5 km from the city of Itu, state of São Paulo, Brazil, at an altitude of ~583 m; the latitudes and longitudes of their sources are shown in Fig. 1.

The AM samples were collected from a hill slope occurring over a wide geographical area, being obtained from thick and homogeneous deposits in easy-to-access topographical locations outside of flood areas. The AC samples were obtained from a horizontal formation at a depth of >30 m, requiring excavation. The samples were homogeneous, obtained from thick deposits gathered by mining. Finally, the AV sample was collected from horizontal layers, requiring excavation. However, the layers are thin and close to the surface, thereby facilitating extraction.

Approximately 150 kg of each raw sample were collected from five different sites in the corresponding quarry locations. Through a quartering process (Tan, 2005), each sample was homogenized and reduced to 80 kg for the laboratory tests. The remaining material was stored in plastic bags.

The samples were dried in a laboratory oven (Deleo, Brazil) at 45 ± 5°C until reaching a constant weight. Once dehydrated, the AM clay was homogenized in a HNTB 100 homogenizer (Natreb, Brazil) and subsequently disaggregated in an LN-15 laboratory roller mill (Natreb, Brazil), while the AC and AV clays were ground for 5 min in a CT-058 hammer mill (Servitech, Brazil) with a 3-mm sieve opening (minimum opening used in an industrial mill).

For the characterization, the clays were ground in a porcelain mortar and passed through a 200-mesh sieve (American Standard Test Sieve Series (ASTM), 74-μm aperture). The chemical analysis of the samples was conducted using X-ray fluorescence (XRF) spectrometry (Bruker S2 Ranger, Germany). The loss on ignition (LOI) of the samples was determined after calcination at 1000°C for 3 h. The mineralogical analysis was conducted using X-ray diffraction (XRD; Bruker D8 Phaser, Germany) with Cu-$K\alpha_1$ radiation ($\lambda = 1.5406$ Å) at 30 kV and 30 mA and at a scanning range of 2–72°2θ and a scanning rate of 2° min^{-1}. Semiquantitative phase quantification was conducted using the rational analysis method. The clay fraction (<2 μm) was determined by employing the NBR 7181 technical standard (ABNT, 2016). Thermogravimetric (TG) analysis was performed in a simultaneous analyser (Netzsch 409 Jupiter F3, Germany) at a heating rate of 10°C min^{-1} from room temperature to 1000°C in synthetic air. The particle-size distribution was determined using laser diffraction (CILAS 1064, France) in the range of 0.04–500 μm for 60 s using sodium salt (PL/G, Lamberti, Brazil) as the dispersant. The residues (i.e. non-silty/clayey material) retained on the 325-mesh sieve (44-μm aperture) after wet sieving were collected and sieved in an electromagnetic shaker (BerTel, Brazil) for 5 min using a set of sieve apertures of 590, 420, 297, 210, 149, 105 and 74 μm.

Clay minerals are negatively charged because of the permanent charges generated by the isomorphic substitutions in the octahedral and tetrahedral sheets and the formation of negative charges at their edges (Ammann *et al.*, 2005). The cation-exchange capacity (CEC) is the ability of the clay to retain cations to balance this negative charge. In this study, CEC was determined using methylene blue adsorption (AFNOR, 1998). The amount of

https://doi.org/10.1180/clm.2023.9 Published online by Cambridge University Press

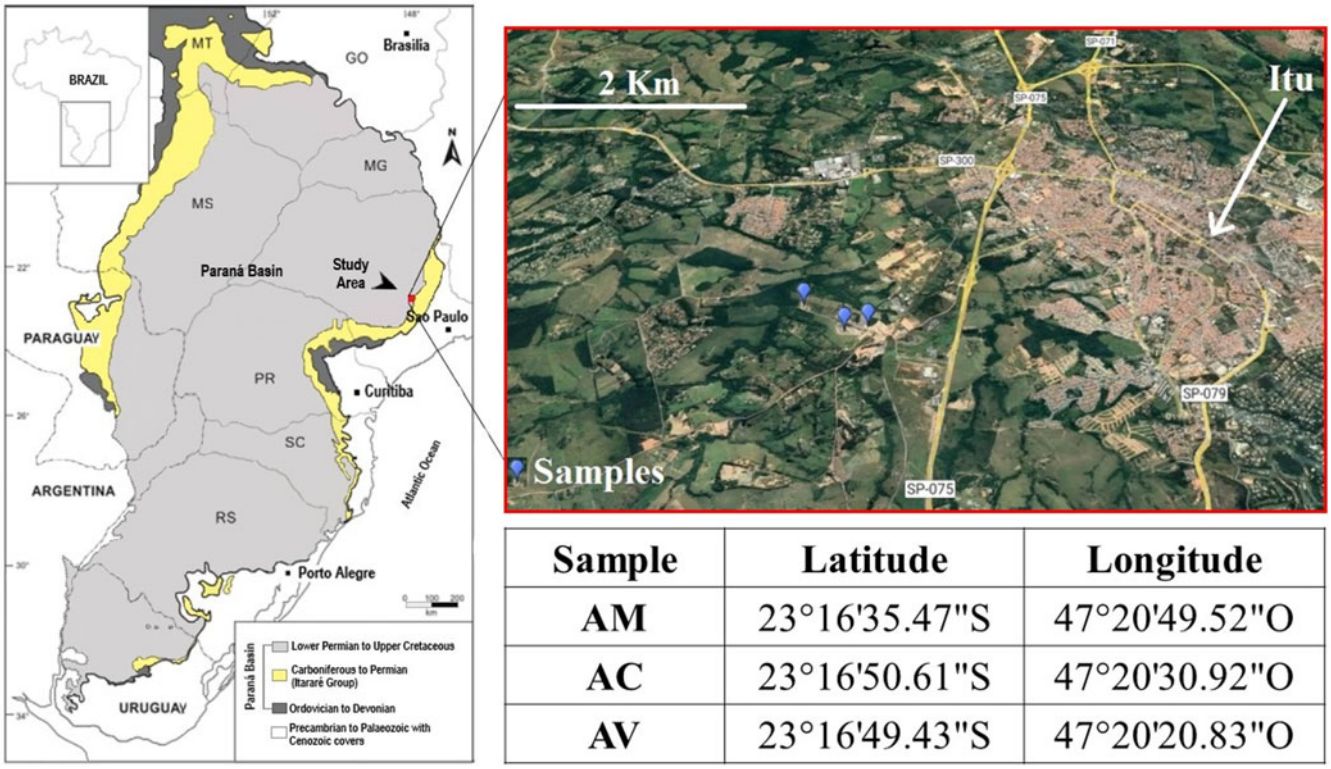

Sample	Latitude	Longitude
AM	23°16'35.47"S	47°20'49.52"O
AC	23°16'50.61"S	47°20'30.92"O
AV	23°16'49.43"S	47°20'20.83"O

Fig. 1. Schematic map of the locations of the leading Brazilian sedimentary basins and collection points of the raw materials used in the study.

methylene blue adsorbed by the clay sample indicates the ability of the clay to adsorb cations from a solution, thereby predicting the reactivity of the clay based on the CEC.

To determine the specific surface area and open pore volume distribution, the clay samples were analysed in powder form, outgassed in a vacuum at 300°C for ~3 h and analysed in a Nova 1200e apparatus (Quantachrome, UK) using liquid nitrogen as the adsorbate. The results were determined using the Brunauer–Emmett–Teller (BET) and Barrett–Joyner–Halenda (BJH) mathematical approaches (Brunauer *et al.*, 1938).

The compositions of the studied clays were determined using the mixture design of experiments (DoE). Formulations of various contents of the studied clays were investigated (Fig. 2). According to the vertices of the diagram in Fig. 2 and the two-way (side) and three-way (centroid) interactions, 10 mixtures were defined, including pure clays (100%), to optimize the mixture design. The mixture design provides an effective mathematical model to predict the properties of the original components and their combinations at specific proportions.

The LL, PL and plasticity index (PI) of the samples were obtained using the indentation method at consistencies (applied forces) of 1 and 46 N for LL and PL, respectively, using a cone penetrometer (Natreb, Brazil).

Analysis of variance (ANOVA) was used to obtain a regression equation for the relationship between the PI experimental data and the content of the used clays in the investigated formulations. The ANOVA was performed using the software *Statistica* v.10 (Statsoft, USA) at a significance level of 95% ($p = 0.05$).

Finally, for the preparation of the Winkler diagram, granulometric analysis of the formulations was carried out by sieving and sedimentation; the latter is appropriate for determining the particle-size distribution of clay-based ceramic compositions based on Stokes' Law (Stokes, 1852) and in accordance with Brazilian standard NBR 7181 (ABNT, 2016). A total of 1 kg of each formulation was dried in an oven at 110 ± 5°C (Solab SL-100, Brazil) and ground to determine the hygroscopic humidity. In this procedure, the samples were sieved to determine particle sizes of between 0.075 and 76 mm. The sieving process was divided into coarse sieving, which refers to the particles retained on the 2.0-mm sieve (10 mesh), and fine sieving, which refers to the particles that passed through the 2.0-mm sieve. The equivalent diameters of the fine fraction of the sample were calculated. Assuming approximately spherical particles, Stokes' Law was applied to relate the sedimentation velocity and particle diameter (NBR 7181; ABNT, 2016). The particle-shedding velocity was obtained indirectly by measuring the suspension density after stirring to achieve homogenization. A densimeter was used to measure the density at regular time intervals. The densimeter reading was correlated with the particle drop height. From these results, a Winkler diagram was employed to help determine which of the studied formulations were suitable for the manufacture of red ceramics.

Results and discussion

Chemistry and mineralogy

Table 1 presents the results of the chemical analysis of the clay samples conducted using XRF spectrometry.

The clays are composed mostly of SiO_2. Clays with SiO_2 contents >70 wt.% are not preferred in ceramics because of their undesirable reactions with other oxides that generate undesirable phases at low firing temperatures (Monsif *et al.*, 2019). The AM clay had the greatest silica content (>66 wt.%), followed by the

https://doi.org/10.1180/clm.2023.9 Published online by Cambridge University Press

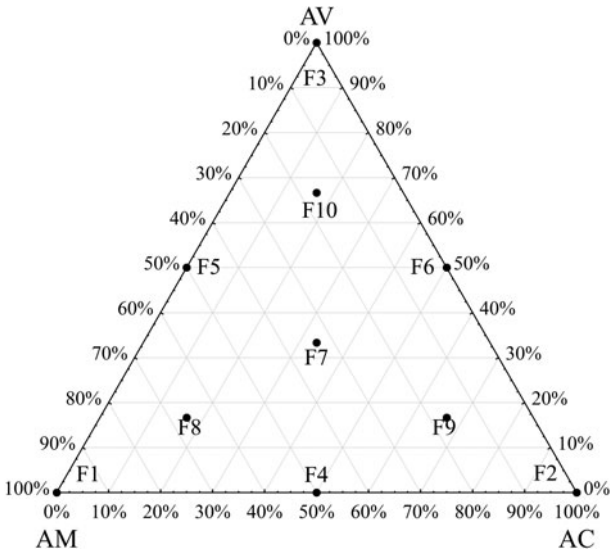

Fig. 2. Triaxial diagram of the developed compositions.

AC clay (62 wt.%) and the AV clay (59 wt.%), which are similar values to those obtained for commonly used raw materials in red ceramic manufacturing (Nandi *et al.*, 2014; Inocente *et al.*, 2017). The raw materials exhibited Fe_2O_3 contents >5 wt.%, which provide a reddish colour after firing, making them suitable for the manufacture of red ceramics (Dondi *et al.*, 2014; Pardo *et al.*, 2018; Harrati *et al.*, 2020). The total content of fluxing agents (Na_2O and K_2O) was >5 wt.% in the AC clay, whereas the contents in the AV and AM clays are >4 and >2 wt.%, respectively. The presence of potassium is attributed mainly to muscovite mica and orthoclase, which occur in the AV clay. These oxides favour the formation of melt during sintering, thereby reducing the porosity and increasing the mechanical strength of the products (Dondi *et al.*, 1999; Cavalcante *et al.*, 2004; Zanelli *et al.*, 2011; Conserva *et al.*, 2017).

The LOI is attributed to the dehydroxylation reactions of silicates, the combustion of organic matter and the decomposition of carbonates (Eliche-Quesada *et al.*, 2018). The LOI values in the studied clays varied between 4.8 and 6.5 wt.%, which are typical values for red ceramics. High LOI values can increase porosity in the ceramic material after sintering (Achik *et al.*, 2021).

The AM and AC clays are rich in quartz (36 and 33 wt.%, respectively), whereas the AV clay has a small quartz content (4 wt.%; Fig. 3 & Table 2). Kaolinite was detected in the AM clay (34 wt.%) and trace montmorillonite was observed in the AV clay. The main minerals that comprise the raw materials are quartz and muscovite mica. Quartz is essential in the drying process because it can act as an auxiliary in the extrusion process, as a deplasticizer that facilitates the extrusion process and as a capillary former that facilitates the fast-drying process (Crozetta *et al.*, 2016).

Table 1. Chemical composition of the clay samples obtained using XRF spectroscopy.

Oxide	Content (wt.%)		
	AM	AC	AV
SiO_2	66.4	62.0	59.0
Al_2O_3	17.1	15.2	18.6
CaO	0.1	2.2	0.4
Fe_2O_3	5.7	5.8	7.3
K_2O	2.4	3.8	4.5
MgO	0.8	3.1	2.5
MnO	0.1	0.1	0.1
Na_2O	0.1	2.1	0.3
P_2O_5	0.1	0.2	0.2
TiO_2	0.8	0.8	0.9
LOI	6.5	4.8	6.3

The thermal analysis curves of the samples show some similarities (Fig. 4). The TG analysis shows the mass losses at temperatures <100°C, corresponding to water evaporation (Nieto *et al.*, 2008). The AV clay exhibits a greater mass loss (~5.5 wt.%), which indicates the significant impact of this temperature range on this clay, affecting the fast-drying process negatively.

The AM and AC clays have smaller mass losses at <100°C (~2 and ~1 wt.%, respectively), which are more suitable for the fast-drying process. In addition, for the AC clay, a greater mass loss (~5 wt.%) was observed in the 300–500°C temperature range.

Particle-size analysis

The particle size of the raw material is essential for optimizing ceramic manufacturing processes, as a suitable particle size eliminates the production of certain defects. This property is fundamental for clays because the mineralogical composition could influence the physical parameters of the raw material. In some cases, the particle size could affect the mechanical strength, permeability and density of the material. Finer particles can promote the packing of particles, thereby increasing the density and mechanical resistance of the material. In addition, such tightly packed particles could reduce water flow from the interior to the surface, thereby inhibiting drying and increasing the duration of the drying cycle significantly. Thus, the particle-size distribution is very relevant to the plasticity of compositions for application in red ceramics (|Monteiro & Vieira, 2004). Figure 5 shows the cumulative particle-size distributions and results curve based on the particle-size distributions of the clay samples.

The AC and AV clays have trimodal distributions, with their first peaks of ~10% of particles having sizes <1 μm. The AM clay exhibits a bimodal behaviour.

As these clay particles are not spherical, the same treatment as that used for spherical particles with lower density values was used to determine the packing density. The results for the particle-size distributions of the raw materials with accumulated fractions of 10, 50 and 90 wt.%, the average particle diameters (D_m) and their size fractions and the amounts of residue (coarse material) retained on the ASTM 325-mesh sieve (44 μm) are shown in Table 3.

The AM clay has a coarser particle-size distribution, with an average particle size >9 μm, whereas the AC and AV clays have similar particle-size distributions. However, the AM clay contains the largest proportion of the <2 μm size fraction; this is also true of the 20–44 μm size fraction. The coarser particles retained on the 325-mesh sieve (>44 μm) can be disaggregated using dispersion equipment.

The coarser particles in the clay (i.e. non-clay materials and sand) facilitate various stages of the production process; thus, they are important to ensuring the quality of the red ceramics by promoting the fast-drying process (Oliveira, 2011). Common impurities in clays, such as quartz, reduce shrinkage because they are non-plastic materials (i.e. they have minimal interactions with moisture and consequently do not cause shrinkage; Crozetta *et al.*, 2016). In the AC clay, 57.7 wt.% of particles were >44 μm,

https://doi.org/10.1180/clm.2023.9 Published online by Cambridge University Press

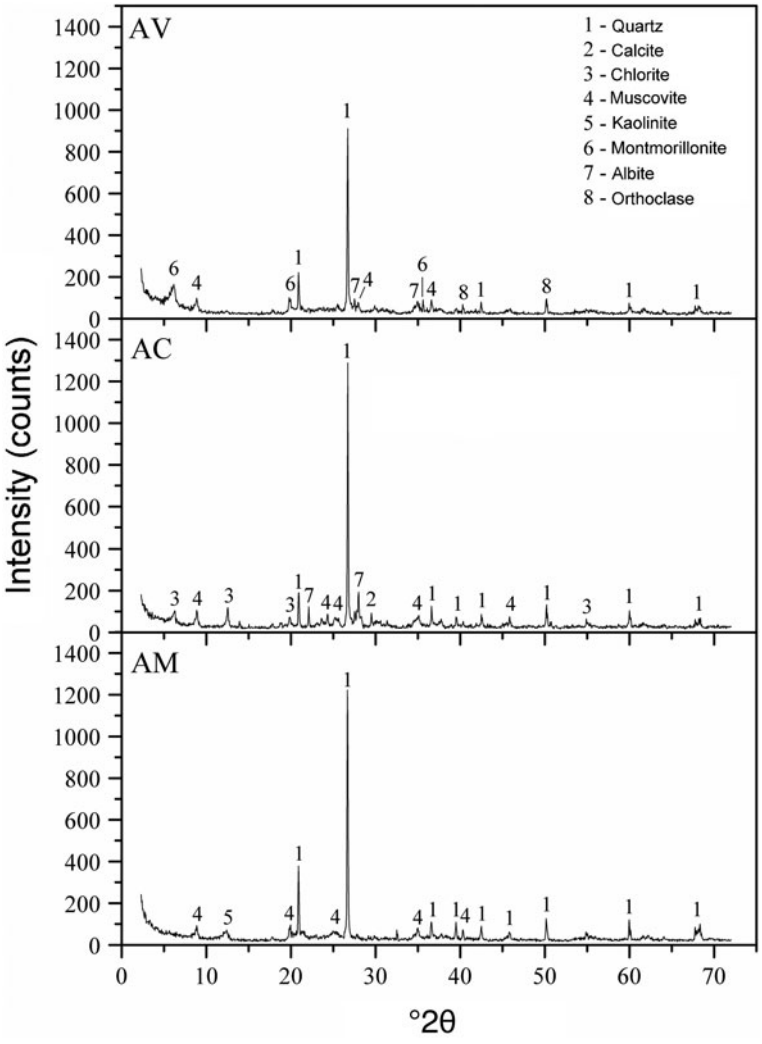

Fig. 3. XRD traces of the investigated clay samples.

which would facilitate the drying process by assisting in the formation of capillaries and promoting water flow. However, excessive amounts of particles of this size could decrease the mechanical strength of such products (Nicolas *et al.*, 2020). Thus, the AV clay was the most plastic due to its small coarse-particle content (7.5 wt.%). The AM clay contained more coarser particles than the AV clay but less than that of the AC clay, which is typical of sandy clays used in the production of red ceramics.

The AC and AV clays were ground in a laboratory hammer mill. However, their great hardness values inhibited fragmentation, rendering them unsuitable for use in traditional red ceramic preparation procedures. Crude residues should have a homogeneous particle-size distribution to facilitate the extrusion and drying stages.

According to the particle-size distribution of the raw waste (Table 4), the AM and AV clay samples were finer because the majority of their waste was finer than 100 mesh. The AC clay had a coarser particle size mainly composed of particles retained in the 50 mesh sieve (>60 wt.%). The coarser-particle contents for the AC and AV clays were influenced by the grinding process, which was standardized, as has been presented previously in this work.

Table 2. Mineralogical composition of the raw materials obtained using XRD analysis.

Sample	Clay fraction (≤2 μm; wt.%)	Mineralogical composition (wt.%)							
		Q	M	C	CH	K	MT	A	O
AM	49.5	36	30	–	–	34	–	–	–
AC	28.2	33	32	2	12	–	–	21	–
AV	50.1	4	79	–	–	–	1	8	8

A = albite; C = calcite; CH = chlorite; K = kaolinite; M = muscovite; MT = montmorillonite; O = orthoclase; Q = quartz.

CEC, specific surface area and pore volume

Figure 6 shows the CEC results obtained from the methylene blue adsorption test compared with the clay mineral contents (Table 1). The AV clay exhibited the greatest CEC due to the abundance of clay minerals in this clay (Tables 2, 3 & 5). A greater clay mineral content results in a greater CEC.

The AV, AM and AC clays consisted of 50.1, 49.5, and 28.2 wt.% clay materials, respectively (Table 2). A greater CEC value results in the adsorption of greater quantities of methylene blue molecules in a given clay mass (Arab *et al.*, 2015).

Although the AM and AV clays had comparable clay contents, the AV clay had a greater CEC, a smaller average particle diameter (Table 3) and the largest specific surface area (Table 5).

https://doi.org/10.1180/clm.2023.9 Published online by Cambridge University Press

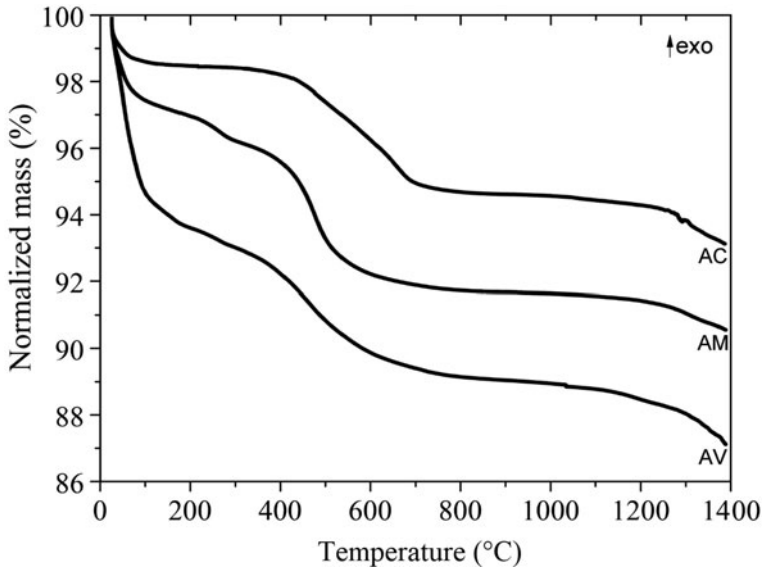

Fig. 4. TG analysis of the investigated clay samples.

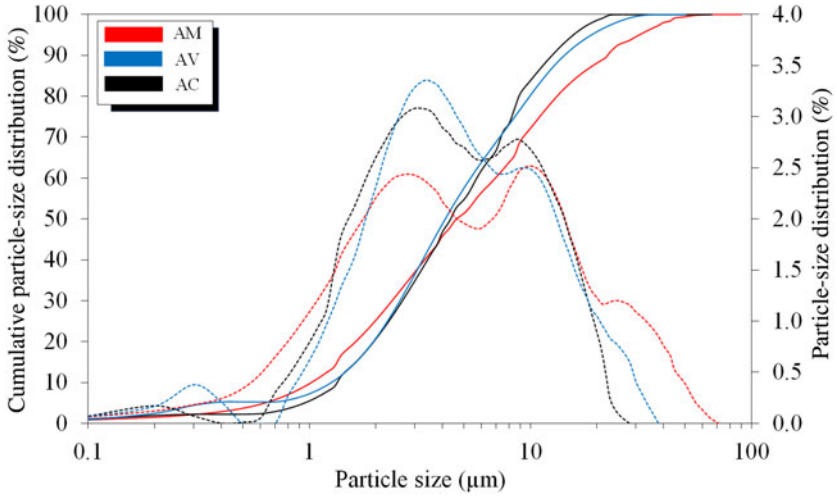

Fig. 5. Cumulative value distribution and particle-size distribution of the raw materials: solid lines = cumulative value distributions; dashed lines = particle-size distributions.

These differences can be ascribed to the particle sizes of the clays (De Kimpe *et al.*, 1979; Petersen *et al.*, 1996; De Jong, 1999). Thus, by correlating the CEC values and mass loss behaviours of the studied raw material samples (Fig. 4), the AV clay, which had the greatest CEC value, had the greatest water loss up to 100°C (~5.5 wt.%), followed by the AM clay (~2 wt.%) and the AC clay (~1 wt.%). In the red ceramic manufacturing process, the great water loss up to 100°C observed for the AV clay, or a material exhibiting similar behaviour, can increase the evaporation rate to too great an extent and lead to the generation of cracks during the fast-drying process; therefore, their content in the ceramic formulation must be moderate or even reduced to zero.

The results regarding the specific surface area of the clay samples are listed in Table 5. The specific surface area is dependent on several variables, such as the type and amount of clay minerals, the CEC and the particle size (De Kimpe *et al.*, 1979; Petersen *et al.*, 1996; De Jong, 1999). The AV clay had the greatest specific surface area, followed by the AM and AC clays. As expected, increasing the clay fraction and decreasing the particle diameter (Tables 1 & 3) increased the specific surface area. A great specific surface area indicates the greater reactivity of the samples, including greater water adsorption on the surfaces of the clay particles (Grohmann, 1972). Thus, by correlating the CEC with the difficulty of water elimination by drying, it can be understood that the AV clay in the formulations should be modified. Moreover, the cumulative volume of BJH desorption from the pores was greater for the AM clay (8.88×10^{-2} cm^3 g^{-1}) and AV clay samples (8.11×10^{-2} cm^3 g^{-1}) than that of the AC clay sample (5.36×10^{-2} cm^3 g^{-1}).

Plasticity of the formulations

The characterization results were used to prepare ten formulations from the studied clays. The experimental process and analysis were performed using the mixture design methodology. The formulations adopted in this study are presented in Fig. 7 and Table 6. The vertices and centroids of the restricted regions in Fig. 2 were analysed to determine the points for the experimental design with complex constraints.

Plasticity is an essential property in the manufacture of red ceramics, indicating the workability of the raw material (Modesto & Bernardin, 2008; Moon, 2016; Spagnoli & Feinendegen, 2017; Baghdad *et al.*, 2019). The plasticity results of the materials determined using the indentation technique are

https://doi.org/10.1180/clm.2023.9 Published online by Cambridge University Press

Table 3. Size distribution (μm), average particle diameter (μm), contents of various sizes (wt.%) and contents of coarser particles (>44 μm; wt.%) of the raw materials.

Raw material	Size distribution (μm)				Content of various sizes (wt.%)			Content of coarser particles (>44 μm; wt.%)
	10%	50%	90%	D_m	<2 μm	2–20 μm	20–44 μm	
AM	1.12	5.03	23.73	9.21	14.59	70.31	15.07	17.10
AC	1.46	4.66	14.50	6.53	12.57	84.66	2.39	57.70
AV	1.26	4.11	14.21	6.24	10.18	84.79	6.09	7.50

Table 4. Retained particles obtained by sieving the raw materials.

Sieve (mesh)	Aperture (μm)	Amount of particles retained (wt.%)		
		AM	AC	AV
30	595	1.43 ± 0.03	27.10 ± 0.99	2.22 ± 0.28
40	420	0.32 ± 0.04	9.57 ± 0.31	0.36 ± 0.08
50	297	0.47 ± 0.04	6.13 ± 0.13	0.34 ± 0.10
70	210	1.21 ± 0.05	5.42 ± 0.18	0.61 ± 0.09
100	149	2.60 ± 0.08	3.79 ± 0.10	0.82 ± 0.08
140	105	3.95 ± 0.06	2.79 ± 0.09	1.20 ± 0.12
200	74	3.21 ± 0.12	1.52 ± 0.06	1.01 ± 0.13
>200	–	3.96 ± 0.12	1.42 ± 0.12	0.99 ± 0.10
Total coarser particles		17.15 ± 0.39	57.74 ± 1.47	7.55 ± 0.36
<44 μm		82.85 ± 0.39	42.26 ± 1.47	92.45 ± 0.36

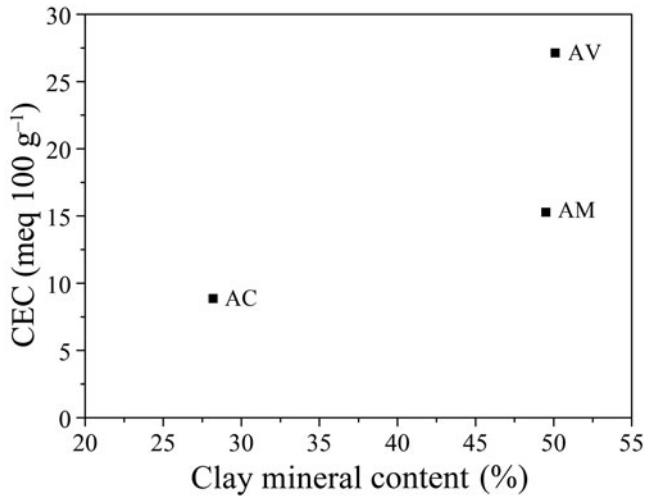

Fig. 6. Correlation between CEC and clay mineral content.

presented in Fig. 7. The LL, PL and PI of the samples were calculated from the equations obtained from the regression analysis and are presented in Table 7.

The water content used for formulation F3 to reach the PL and LL was significantly greater than those for the other formulations. As formulation F3 corresponds to 100 wt.% AV clay, the greater specific surface area and CEC indicate a greater amount of water to be needed in the forming process by extrusion. In contrast, the opposite behaviour was observed for formulation F2 (100 wt.% AC clay), which has the smallest specific surface area and CEC. Clays with greater plasticity have less resistance to deformation because plastic clays need greater water contents

Table 5. Specific surface areas and pore volumes of the clay samples.

	AM	AC	AV
Specific surface area ($m^2\ g^{-1}$)	36.27	20.79	45.92
Total pore volume ($cm^3\ g^{-1}$)	8.88×10^{-2}	5.36×10^{-2}	8.11×10^{-2}

for moulding. Plasticity occurs because of the lubricating action of water between the lamellar particles of clays (Modesto & Bernardin, 2008). Clays with greater water contents could develop cracks during drying.

Oliveira (2011) purposed the following classification of clays according to their PI:

- $0 < PI < 1$: non-plastic clays
- $1 < PI < 7$: low-plasticity clays
- $7 < PI < 15$: moderate-plasticity clays
- $PI > 15$: high-plasticity clays

However, Moreno-Maroto & Alonso-Azcárate (2018) introduced a new parameter to evaluate the plasticity of clays: the PI/LL ratio. Clays with a PI/LL ratio ≤ 0.33 can be considered low-plasticity clays, those with a PI/LL ratio < 0.33 and >0.5 are moderate-plasticity clays and those with a PI/LL ratio >0.5 are high-plasticity clays.

The plasticity classifications of the formulations studied according to Oliveira (2011) and Moreno-Maroto & Alonso-Azcárate (2018) are presented in Table 7. These classifications are very good indications of clay plasticity. There were some acceptable differences between classifications depending on the used criteria, demonstrating the complexity of defining a parameter that indicates the best clay to be used in a given process. According to the classification of Moreno-Maroto & Alonso-Azcárate (2018), all investigated formulations in our work could be used in red ceramic manufacturing, except formulation F1 (high plasticity) and excluding formulations F2 and F3 as these were pure clays. Therefore, other criteria needed to be used in our work to determine the best potential formulations for fast-drying red ceramics.

The interaction with water and the workability of the formulation decreased as the plastic content with deformation resistance of the clay decreased. Most of these clays contained abundant minerals that adsorb small amounts of water on the particle surface, such as quartz. Thus, moisture variations, although small, resulted in significant variation in the force required for indentation/deformation.

The results obtained were validated by statistical analysis. Table 8 shows the PI results obtained through ANOVA and plotted as a response surface (Fig. 8). A reliability threshold of 95% was employed. For the analysis, a higher *F*-value indicates greater significance and a lower *p*-value suggests greater reliability.

The plasticity of clays is influenced in a complex way by their mineralogical and granulometric characteristics. This makes it difficult to predict the LL and PL values of a clay material based on its composition; at most, it is possible to identify general trends that can provide indications of the degree of workability (Marsigli & Dondi, 1997). The PI tended to increase as AM clay was incorporated into the mixtures, whereas the AV and AC clays were plasticity reducers.

https://doi.org/10.1180/clm.2023.9 Published online by Cambridge University Press

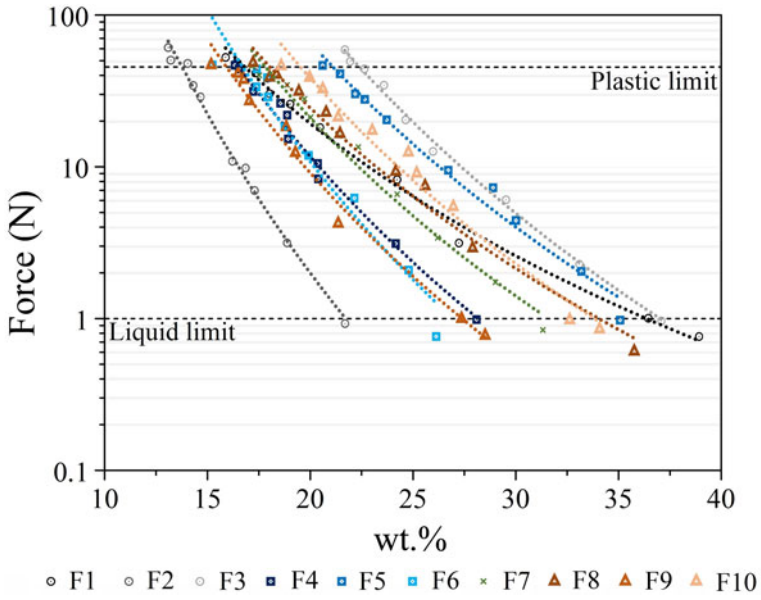

Fig. 7. Force (N) applied for the indentation of the formulations as a function of the water content (wt.%).

Table 6. Clay ceramic formulations (mixtures; wt.%) using the selected raw materials according to the mixture design.

Formulation	Clay content (wt.%)		
	AM	AC	AV
F1	100.0	0.0	0.0
F2	0.0	100.0	0.0
F3	0.0	0.0	100.0
F4	50.0	50.0	0.0
F5	50.0	0.0	50.0
F6	0.0	50.0	50.0
F7	33.4	33.3	33.3
F8	66.6	16.7	16.7
F9	16.7	66.6	16.7
F10	16.7	16.7	66.6

Equation 1 shows the mathematical expression that best fits the PI and clay content experimental data for the raw materials and formulations investigated in this work:

$$PI = 18.502x + 7.720y + 14.312z \quad (1)$$

where x is the AM clay content (wt.%), y is the AV clay content (wt.%) and z is the AC clay content (wt.%).

Figure 9 presents the classification of the extrusion of the studied formulations in a Holtz and Kovacs diagram (Fig. 9a) and according to their extrusion workability (Fig. 9b). Although the graphs in Fig. 9 have been developed for PL and LL values obtained using the Atterberg method, our experimental data, obtained using the indentation method, fit these graphs very well.

Figure 9a shows a Holtz and Kovacs diagram (i.e. PI as a function of the LL of the investigated formulations; Holtz & Kovacs, 1981). All of the prepared formulations are classified within the low- and moderate-plasticity fields, including the F1, F2 and F3 formulations, (pure AM, AC and AV clays, respectively). The F1 formulation (AM clay) exhibited the greatest PI value and behaved as an illite and montmorillonite clay, although these minerals were not present in its composition. This might be explained by the presence of muscovite mica that is similar to illite and the lack of low-plasticity minerals, such as albite and orthoclase, although significant amounts of quartz were present. The F3, F5 and F8 formulations are within the illite clay area of the diagram. Thus, they are considered formulations of greater

Table 7. Regression equation, PL, LL, PI and PI/LL ratio values and corresponding classification of each studied formulation according to Oliveira (2011) and Moreno-Maroto & Alonso-Azcárate (2018).

Formulation	Equation[a]	PL (%)	LL (%)	PI (%)	PI/LL ratio	Plasticity classification	
						Oliveira (2011)	Moreno-Maroto & Alonso-Azcárate (2018)
F1	$F = 5 \times 10^{7}\ W^{-4.954}$	16.54	35.82	19.28	0.54	High	High
F2	$F = 2 \times 10^{11}\ W^{-8.378}$	14.14	22.33	8.19	0.37	Moderate	Moderate
F3	$F = 8 \times 10^{11}\ W^{-7.597}$	22.28	36.88	14.60	0.40	Moderate	Moderate
F4	$F = 3 \times 10^{10}\ W^{-7.176}$	16.92	28.84	11.93	0.41	Moderate	Moderate
F5	$F = 6 \times 10^{10}\ W^{-6.908}$	20.87	36.33	15.46	0.43	High	Moderate
F6	$F = 3 \times 10^{11}\ W^{-8.011}$	16.79	27.08	10.29	0.38	Moderate	Moderate
F7	$F = 1 \times 10^{10}\ W^{-6.666}$	17.81	31.63	13.82	0.44	Moderate	Moderate
F8	$F = 2 \times 10^{9}\ W^{-6.012}$	18.64	35.24	16.60	0.47	High	Moderate
F9	$F = 9 \times 10^{9}\ W^{-6.929}$	15.73	27.33	11.60	0.42	Moderate	Moderate
F10	$F = 4 \times 10^{10}\ W^{-6.952}$	19.31	33.50	14.19	0.42	Moderate	Moderate

[a]Mathematical expressions were obtained using *Excel*™ software.
F = force; W = water content.

https://doi.org/10.1180/clm.2023.9 Published online by Cambridge University Press

Table 8. ANOVA of the PI values of the investigated formulations.

PI	SS effect	df effect	MS effect	*F*	*p*	R^2	R^2 adjusted
Linear	**88.63**	**2**	**44.32**	**39.03**	**0.00**	**0.92**	**0.89**
Quadratic	1.78	3	0.59	0.38	0.77	0.94	0.86
Special cubic	4.76	1	4.76	10.13	0.05	0.99	0.96
Cubic	0.42	2	0.21	0.21	0.84	0.99	0.91
Total adjusted	96.58	9	10.73	–	–	–	–

The model that is statistically significant with 95% confidence (i.e. $p < 0.05$) is highlighted in bold.
df = degrees of freedom; MS = mean squares; SS = sum of squares.

plasticity than formulation F1. The low PI values of the F2, F4, F6 and F9 formulations are related to their greater feldspar (albite) content and AC clay contents of 100.0, 50.0, 50.0 and 66.6 wt.%, respectively.

Formulations F2, F4, F6 and F9 are in the region of low-plasticity clays. The PI/LL ratio values (Moreno-Maroto & Alonso-Azcárate, 2018) were: F2 = 0.37, F4 = 0.41, F6 = 0.38 and F9 = 0.42 (Table 7). Formulations F2 and F6 (lower PI/LL ratio values) are farther from the region comprising moderate-plasticity clays, while formulations F4 and F9 are closer to this region, as they have greater PI/LL ratios.

The plastic properties of the clay samples are indicated in the extrusion workability factor graph (Casagrande, 1932; Casagrande, 1948; Gippini, 1969) in Fig. 9b. This diagram shows two ranges of plasticity values: an optimal and an acceptable one for processing of the clayey material. This means that we would be able to achieve high extrusion quality during industrial processes with these clays (Marsigli & Dondi, 1997). This may serve as a basis for defining and optimizing the formulations that could be used for the fast-drying process. The PI value is essential to determining the applicability of such formulations. Formulations F7 and F10 exhibited good extrusion behaviour and formulation F3, which corresponds to the pure AV clay, had acceptable extrusion properties. However, working with only one clay is not recommended during production processes. Thus, the formulations should be corrected before defects can develop during the manufacturing process. In Fig. 9b, only formulations F5 and F8 are present within the optimal extrusion zone (Gippini, 1969), indicating that they would be easy to work with, thereby improving the extrusion process and enabling great productivity (Marsigli & Dondi, 1997).

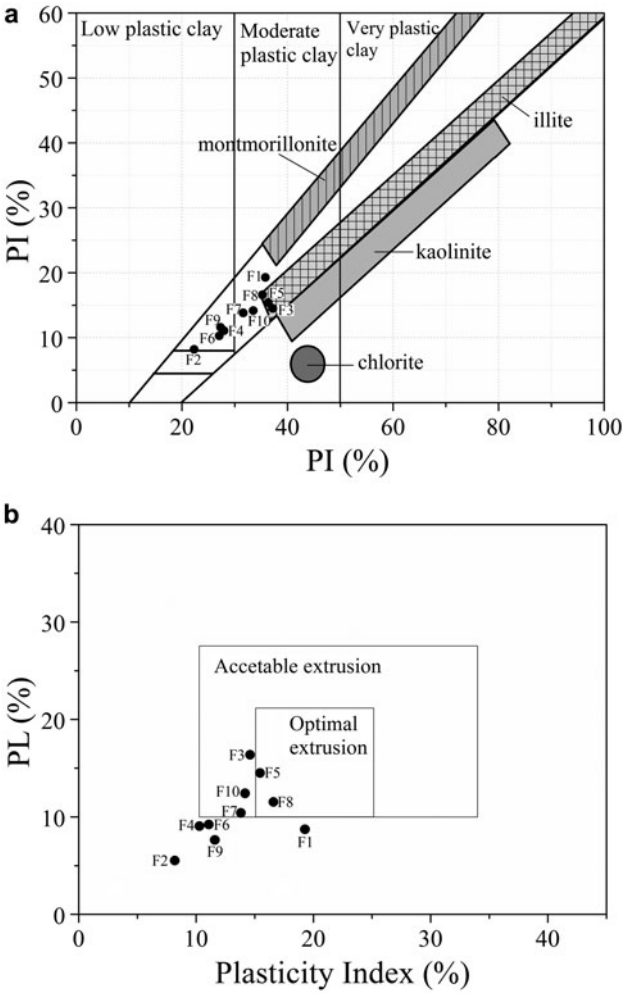

Fig. 9. Classification for the extrusion of the formulations: (a) on the Holtz and Kovacs diagram and (b) according to extrusion workability.

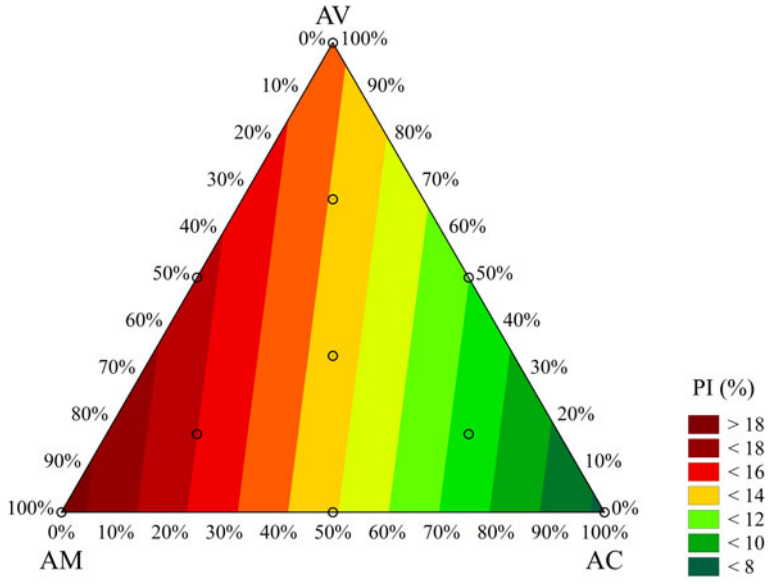

Fig. 8. PI response surface for the formulations studied (F1–F10).

https://doi.org/10.1180/clm.2023.9 Published online by Cambridge University Press

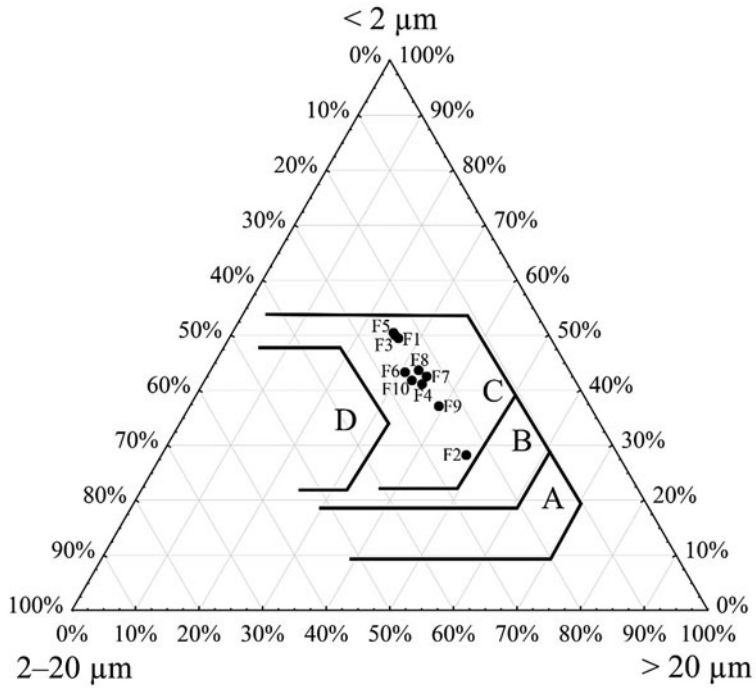

Fig. 10. Projection of the clay formulations on a Winkler diagram (Winkler, 1954). The fields are defined as follows: A = standard bricks; B = vertically perforated bricks; C = tiles and masonry bricks; D = hollow bricks.

Thus, when the PL and PI data obtained using the indentation method were used to evaluate the extrusion workability factor (Fig. 9b), similar results as discussed previously were observed. Formulations F3, F5, F7, F8 and F10 could be used in extrusion; however, the use of formulation F3 would not be recommended, as it consists only of one clay (AV clay). Therefore, the graphs in Fig. 9 could be helpful, within an acceptable margin of safety, when choosing formulations with the greatest possibility of being used successfully in extrusion.

Figure 10 shows the suitability of the prepared formulations for obtaining ceramic products based on the Winkler diagram, which is an essential tool for use when processing red ceramics (Winkler, 1954).

Based on the particle-size distributions of the clays, the manufacture of specific types of products and mixing of raw materials can be achieved. Clay minerals and formulations located close to the apex in Fig. 10 for the <2 µm fraction have greater plasticity. Greater plasticity is advantageous because it increases the mechanical strength of the material and decreases wear on the stock preparation and production equipment. However, formulations with greater plasticity require more water, rendering the drying stage difficult and increasing the energy demand to remove the structural water from the clay minerals during the firing stage. According to these results, all of the prepared formulations are suitable for manufacturing masonry bricks and tiles (Strazzera *et al.*, 1997; Semiz, 2017).

The technique of using DoE and ANOVA for the formulation of ceramic compositions from the studied clays was adequate for the analysis of plasticity behaviour during extrusion. Through the extrusion workability factor, it was possible to define the formulations that could be used for the fast-drying process, as only the formulations that presented optimal and acceptable extrusion conditions could be used. In this study, four formulations were selected (F5, F7, F8 and F10), which, according to the plasticity analysis and the Winkler diagram, are suitable for the manufacture of fast-drying red ceramics.

Summary and conclusions

This work assessed three clay raw materials from Itu, São Paulo, Brazil, for the manufacture of fast-drying red ceramics. The clays consisted principally of SiO_2, Al_2O_3, Fe_2O_3, K_2O and MgO and contained abundant muscovite mica, quartz, kaolinite and albite. All of the clay samples had Fe_2O_3 contents >5 wt.%, which provides the reddish colours of the ceramics. The Al_2O_3/SiO_2 ratios indicated significant clay mineral contents. The formulations with AM and AC clay contents exhibited great plasticity. The AC clay was more suitable for the preparation of red ceramic formulations for fast drying. The greater content of coarser particles of this clay (57.74%) compared to its AM and AV clay counterparts (17.15% and 7.55%, respectively) increased the permeability of the material and facilitated drying. Among the 10 prepared formulations, formulation F5 (50.0 wt.% AM clay and 50.0 wt.% AV clay), formulation F7 (33.3 wt.% AM clay, 33.3 wt.% AC clay and 33.3 wt.% AV clay), formulation F8 (66.6 wt.% AM clay, 16.7 wt.% AC clay and 16.7 wt.% AV clay) and formulation F10 (16.7 wt.% AM clay, 16.7 wt.% AC clay and 66.6 wt.% AV clay) presented the most appropriate PL and PI values within the acceptable levels for extrusion. Through the extrusion workability factor, it was possible to determine the formulations that could be used in the fast-drying process, as only the formulations that presented optimal and acceptable extrusion conditions can be used for this purpose. Four formulations were selected (F5, F7, F8 and F10), which, according to the plasticity analysis and the Winkler diagram, are suitable for the manufacture of fast-drying red ceramics. Therefore, this study provided notable findings on the development of red ceramic formulations processed by extrusion for the manufacture of fast-drying red ceramics. Although every company that manufactures red ceramics uses clays with varying characteristics from those used in this study, the evaluation based on the chemical, mineralogical and granulometric composition and the methodology for determining the PI can be used as a guide for determining the composition

https://doi.org/10.1180/clm.2023.9 Published online by Cambridge University Press

necessary to allow formation by extrusion in the manufacture of fast-drying red ceramics.

Financial support. The authors thank the Coordination for Higher Education Improvement (CAPES/Brazil, processes no. 88887.502321/2020-00 and 88887.356961/2019-00) and the National Council for Scientific and Technological Development (CNPq/Brazil, processes no. 306992/2019-1, 307761/2019-3, 310328/2020-9 and 304054/2021-6) for the financial support of this work.

Supplementary material. To view supplementary material for this article, please visit https://doi.org/10.1180/clm.2023.9.

References

ABNT (2016) *NBR 7181: Soil – Granulometric Analysis*. Brazilian Association of Technical Standards, Rio de Janeiro, Brazil, 3 pp.

Achik M., Benmoussa H., Oulmekki A., Ijjaali M., Moudden N.E. *et al.* (2021) Evaluation of technological properties of fired clay bricks containing pyrrhotite ash. *Construction & Building Materials*, **269**, 121312.

AFNOR (1998) *NF P94-068 – Sols: reconnaissance et essais – Mesure de la capacité d'adsorption de bleu de méthylène d'un sol ou d'un matériau rocheux – Détermination de la valeur de bleu de méthylène d'un sol ou d'un matériau rocheux par l'essai à la tache*. French Association of Normalization, Saint-Denis, France, 8 pp.

Aghayev T. & Küçükuysal C. (2018) Ceramic properties of Uşak clay in comparison with Ukrainian clay. *Clay Minerals*, **53**, 549–562.

Ammann L., Bergaya F. & Lagaly G. (2005) Determination of the cation exchange capacity of clays with copper complexes revisited. *Clay Minerals*, **40**, 441–453.

Andrade F.A., Al-Qureshi H.A. & Hotza D. (2011) Measuring the plasticity of clays: a review. *Applied Clay Science*, **51**, 1–7.

Arab P.B., Araújo T.P. & Pejon O.J. (2015) Identification of clay minerals in mixtures subjected to differential thermal and thermogravimetry analyses and methylene blue adsorption tests. *Applied Clay Science*, **114**, 133–140.

Baghdad A., Bouazi R., Bouftouha Y., Hatert F. & Fagel N. (2019) Characteristics and firing behaviour of the under-Numidian clay deposits from the Jijel region (northeast Algeria): potential use in the ceramics industry. *Clay Minerals*, **54**, 325–337.

Brunauer S., Emmett P.H. & Teller E. (1938) Adsorption of gases in multimolecular layers. *Journal of the American Chemical Society*, **60**, 309–319.

Cabral Junior M., Tanno L.C., Sintoni A., Motta J.F.M. & Coelho J.M. (2012) A indústria de cerâmica vermelha e o suprimento mineral no Brasil: desafios para o Aprimoramento da competitividade. *Cerâmica Industrial*, **17**, 36–42.

Casagrande A. (1932) Research on the Atterberg limits of soils. *Public Roads*, **13**, 121–146.

Casagrande A. (1948) Classification and identification of soils. *Transactions of the American Society of Civil Engineers*, **113**, 901–991.

Cavalcante P.M.T., Dondi M., Ercolani G., Guarini G., Melandri C., Raimondo M. & Rocha e Almendra E. (2004) The influence of microstructure on the performance of white porcelain stoneware. *Ceramics International*, **30**, 953–963.

Conserva L.R.S., Melchiades F.G., Nastri S., Boschi A.O., Dondi M., Guarini G. *et al.* (2017) Pyroplastic deformation of porcelain stoneware tiles: wet *vs*. dry processing. *Journal of the European Ceramic Society*, **37**, 333–342.

Crozetta J.R., Nandi V.S., Rosso F., Zaccaron A. & Niero D.F. (2016) Influência de tamanhos de partículas na plasticidade e retração de secagem das argilas. *Cerâmica Industrial*, **21**, 21–29.

Deboucha S. & Hashim R. (2011) A review on bricks and stabilized compressed earth blocks. *Scientific Research Essays*, **6**, 499–506.

De Jong E. (1999) Comparison of three methods of measuring surface area of soils. *Canadian Journal of Soil Science*, **79**, 345–351.

De Kimpe C.R., Laverdiere M.R. & Martel Y.A. (1979) Surface area and exchange capacity of clay in relation to the mineralogical composition of gleysolic soils. *Canadian Journal of Soil Science*, **59**, 341–347.

Doménech V., Sánchez E., Sanz V., García J. & Ginés F. (1994) Assessing the plasticity of ceramic masses by determining indentation force. Pp. 59–69 in: *III World Congress on Ceramic Tile Quality. General Lectures and Open Papers II*. Castellón, Spain: Qualicer.

Dondi M., Ercolani G., Melandri C., Mingazzini C. & Marsigli M. (1999) The chemical composition of porcelain stoneware tiles and its influence on microstructure and mechanical properties. *InterCeram: International Ceramic Review*, **48**, 75–83.

Dondi M., Raimondo M. & Zanelli C. (2014) Clays and bodies for ceramic tiles: reappraisal and technological classification. *Applied Clay Science*, **96**, 91–109.

Eliche-Quesada D., Sandalio-Pérez J.A., Martínez-Martínez S., Pérez-Villarejo L. & Sánchez-Soto P.J. (2018) Investigation of use of coal fly ash in eco-friendly construction materials: fired clay bricks and silica-calcareous non fired bricks. *Ceramics International*, **44**, 4400–4412.

Gippini E. (1969) Contribution à l'ètude des proprietés de molage des argiles et des mèlanges optimaux de matières premières. *L'Industrie Céramique*, **619**, 423–435.

Grohmann F. (1972) Superfície específica do solo de unidades de mapeamento do estado de São Paulo: I – Estudo de perfis com horizonte B textural e horizonte B latossólico. *Bragantia*, **31**, 145–165.

Harrati A., Manni A., Hassani F.O., Sdiri A., Kalakhi S.E., Bouari A. *et al.* (2020) Potentiality of new dark clay-rich materials for porous ceramic applications in Ouled Sidi Ali Ben Youssef Area (coastal Meseta, Morocco). *Boletín de la Sociedad Española de Cerámica y Vidrio*, **61**, 130–145.

Holtz R.D. & Kovacs W.D. (1981) *An Introduction to Geotechnical Engineering*, 1st edition. Prentice Hall, Hoboken, NJ, USA, 733 pp.

Inocente J.M., Nandi V.S., Rosso F., de Oliveira A. & Zaccaron A. (2017) Study for vitreous waste recovery in the formulation of heavy clay ceramics. *Materials Science & Engineering International Journal Research*, **1**, 56–60.

Jemaï M.B.M., Karoui-Yaakoub N., Sdiri A., Salah I.B., Azouzi R. & Duplay J. (2015) Late Cretaceous and Palaeocene clays of the northern Tunisia: potential use for manufacturing clay products. *Arabian Journal of Geoscience*, **8**, 11135–11148.

Cabral Júnior M., Motta J.F.M., Almeida A.S. & Tanno L.C. (2008) Argila para cerâmica vermelha. Pp. 747–770 in: *Rochas e Minerais Industriais no Brasil: usos e especificações* (A.B. Luz & F.A.F. Lins, editors). CETEM/MCTI, Rio de Janeiro, Brazil.

Karakan E. (2022a) Comparative analysis of Atterberg limits, liquidity index, flow index and undrained shear strength behavior in binary clay mixtures. *Applied Sciences*, **12**, 8616.

Karakan E. (2022b) Relationships among plasticity clay fraction and activity of clay sand mixtures. *Arabian Journal of Geosciences*, **15**, 334.

Karakan E. & Demir S. (2018) Effect of fines content and plasticity on undrained shear strength of quartz–clay mixtures. *Arabian Journal of Geosciences*, **11**, 743.

Karakan E. & Demir S. (2020) Observations and findings on mechanical and plasticity behavior of sand–clay mixtures. *Arabian Journal of Geosciences*, **13**, 983.

Karakan E., Shimobe S. & Sezer A. (2020) Effect of clay fraction and mineralogy on fall cone results of clay–sand mixtures. *Engineering Geology*, **279**, 105887.

Kazmi S.M.S., Abbas S., Saleem M.A., Munir M.J. & Khitab A. (2016) Manufacturing of sustainable clay bricks: utilization of waste sugarcane bagasse and rice husk ashes. *Construction & Building Materials*, **120**, 29–41.

Ketelaars A.A.J., Pel L., Coumans W.J. & Kerkhof P.J.A.M. (1995) Drying kinetics: a comparison of diffusion coefficients from moisture concentration profiles and drying curves. *Chemical Engineering Science*, **50**, 1187–1191.

Ben Mabrouk S. & Belghith A.A. (1995) Numerical simulation of the drying of a derfomable material: evolution of the diffusion coefficient, *Drying Technology*, **13**, 1789–1805.

Marsigli M. & Dondi M. (1997) Plasticitá delle argille Italiane per laterizi e previsione del loro comportamento in foggiatura. *L'Industria dei Laterizi*, **46**, 214–222.

MME (2022) Plano Nacional de Mineração 2030. Retrieved from: http://antigo.mme.gov.br/web/guest/secretarias/geologia-mineracao-e-transformacao-mineral/destaques-do-setor-de-energia/plano-nacional-de-mineracao-2030.

Modesto C.O. & Bernardin A.M. (2008) Determination of clay plasticity: Indentation method *versus* Pfefferkorn method. *Applied Clay Science*, **40**, 15–19.

Monsif M., Zerouale A., Idrissi Kandri N., Mozzon M., Sgarbossa P., Zorzi F. *et al.* (2019) Chemical–physical and mineralogical characterization of

ceramic raw materials from Moroccan northern regions: intriguing resources for industrial applications. *Applied Clay Science*, **182**, 105274.
Monteiro S.N. & Vieira C.M.F. (2004) Influence of firing temperature on the ceramic properties of clays from Campos dos Goytacazes, Brazil. *Applied Clay Science*, **27**, 229–234.
Moon V. (2016) Halloysite behaving badly: geomechanics and slope behaviour of halloysite-rich soils. *Clay Minerals*, **51**, 517–528.
Moreno-Maroto J.M. & Alonso-Azcárate J. (2018) What is clay? A new definition of 'clay' based on plasticity and its impact on the most widespread soil classification systems. *Applied Clay Science*, **161**, 57–63.
Muñoz V.P., Morales O.M.P., Letelier G.V. & Mendívil G.M.A. (2016) Fired clay bricks made by adding wastes: assessment of the impact on physical, mechanical and thermal properties. *Construction & Building Materials*, **125**, 241–252.
Nandi V.S., Zaccaron A., Fernandes P., Dagostin J.P. & Bernardin A.M. (2014) Adição de vidro reciclado de Lâmpadas na fabricação de cerâmica vermelha. *Cerâmica Industrial*, **19**, 29–32.
Nicolas M.F., Vlasova M., Aguilar P.A.M., Kakazey M., Cano M.M.C., Matus R.A. & Puig T.P. (2020) Development of an energy-saving technology for sintering of bricks from high-siliceous clay by the plastic molding method. *Construction & Building Materials*, **242**, 118142.
Nield D.A. & Simmons C.T. (2019) A brief introduction to convection in porous media. *Transport in Porous Media*, **130**, 237–250.
Nieto F., Abad I. & Azañón J.M. (2008) Smectite quantification in sediments and soils by thermogravimetric analyses. *Applied Clay Science*, **38**, 288–296.
Oliveira A.A. (2011) *Tecnologia em Cerâmica*. Editora Lara, Criciúma, Brazil, 176 pp.
Pardo F., Jordan M.M. & Montero M.A. (2018) Ceramic behaviour of clays in central Chile. *Applied Clay Science*, **157**, 158–164.
Petersen L.W., Moldrup P., Jacobsen O.H. & Rolston D.E. (1996) Relations between specific surface area and soil physical and chemical properties. *Soil Science*, **161**, 9–21.
Schaefer C.E.G.R., Fabris J.D. & Ker J.C. (2008) Minerals in the clay fraction of Brazilian Latosols (Oxisols): a review. *Clay Minerals*, **43**, 137–154.
Semiz B. (2017) Characteristics of clay-rich raw materials for ceramic applications in Denizli region (western Anatolia). *Applied Clay Science*, **137**, 83–93.
Shakir A.A. & Mohammed A.A. (2013) Manufacturing of bricks in the past, in the present and in the future: a state of the art review. *International Journal of Advances in Applied Science*, **2**, 145–156.
Spagnoli G. & Feinendegen M. (2017) Relationship between measured plastic limit and plastic limit estimated from undrained shear strength, water content ratio and liquidity index. *Clay Minerals*, **52**, 509–519.
Stokes G.G. (1852) *On the Composition and Resolution of Streams of Polarized Light from Different Sources. Proceedings of the Cambridge Philosophical Society: Mathematical and physical sciences, Transactions of the Cambridge Philosophical Society*, 9th edition. Cambridge University Press, Cambridge, UK, 399 pp.
Strazzera B., Dondi M. & Marsigli M. (1997) Composition and ceramic properties of tertiary clays from southern Sardinia (Italy). *Applied Clay Science*, **12**, 247–266.
Tan K.H. (2005) *Soil Sampling, Preparation, and Analysis*. CRC Press, Boca Raton, FL, USA, 672 pp.
Toei R. (1985) Giants of drying. *Drying Technology*, **3**, 1–14.
Toei R., Okazaki M. & Tamon, H. (1994) Conventional basic design for convection or conduction dryers. *Drying Technology*, **12**, 59–97.
Ukwatta A., Mohajerani A., Setunge S. & Eshtiaghi N. (2015) Possible use of biosolids in fired-clay bricks. *Construction & Building Materials*, **91**, 86–93.
Vasconcellos A.M., Sousa S.R., Moura S.R., Silva N.J.B., Gomes S.W.R. & Barbosa L.A.G. (2019) Drying of industrial hollow ceramic brick: a numerical analysis using CFD. *Defect and Diffusion Forum*, **391**, 48–53.
Winkler H.G.F. (1954) Bedeutung der Korngrößenverteilung und des Mineralbestandes von Tonen für die Herstellung grobkeramischer Erzeugnisse. *Berichte Deutche Keramics Gesellschaft*, **31**, 337–343.
Zaccaron A., Nandi V.S. & Bernardin A.M. (2021) Fast drying for the manufacturing of clay ceramics using natural clays. *Journal of Building Engineering*, **33**, 101877.
Zaccaron A., Nandi V.S., Dal Bó M., Arcaro S. & Bernardin A.M. (2022) The behavior of different clays subjected to a fast-drying cycle for traditional ceramic manufacturing. *Journal of King Saud University – Engineering Sciences* (in press).
Zanden V.A.J.J. (1996) Modelling and simulating simultaneous liquid and vapour transport in partially saturated porous materials. Pp. 157–177 in: *Mathematical Modelling and Numerical Techniques in Drying Technology*. Marcel Dekker, Inc., New York, NY, USA.
Zanelli C., Raimondo M., Guarini G. & Dondi M. (2011) The vitreous phase of porcelain stoneware: composition, evolution during sintering and physical properties. *Journal of Non-Crystalline Solids*, **357**, 3251–3260.

https://doi.org/10.1180/clm.2023.9 Published online by Cambridge University Press